Water Supply

Water Supply Vol 24 No 8, 2946 doi: 10.2166/ws.2024.182

Spatial and seasonal assessment of surface water quality for domestic use in a semi-arid area of the Upper Kebir Sub-basin, NE Algeria

Zineb Allia[a,b], Meryem Lalaoui[b,c] and Mohamed Chebbah[b,c,*]

[a] Institute of Science and Technology, University Center of A. Boussouf Mila, BP 26 RP, Mila 43000, Algeria
[b] Institute of Life and Nature Sciences, University Center of A. Boussouf Mila, BP 26 RP, Mila 43000, Algeria
[c] Natural Sciences & Materials Laboratory, LSNM, University Center of A. Boussouf Mila, BP 26 RP, Mila 43000, Algeria
*Corresponding author. E-mail: m.chebbah@centre-univ-mila.dz

MC, 0000-0001-5285-3767

ABSTRACT

The present study was conducted out in the Upper Kebir Sub-basin [North East (NE) Algeria] aiming to evaluate the status and spatial–seasonal variability of water quality for domestic purposes using hydrogeochemical parameters and water quality indices. Surface water samples were collected from 27 selected sites, in 2020–2021 during both the wet and dry seasons and were analysed for 22 parameters. The findings were compared with WHO standards and the water quality indices were calculated. The analysis revealed that the basin was mainly polluted and showed significant seasonal and spatial variations in water quality, considerably influenced by climatic conditions (surface runoff) and human activities (urban sewage and agricultural activities). The results reveal significant spatio-temporal fluctuations and highlight areas likely to be affected by anthropogenic activities.

Key words: Algeria, domestic use, heavy metals, surface water, water quality

HIGHLIGHTS

- The assessment highlights substantial spatial-seasonal fluctuations in water quality, with a marked deterioration during the dry season.
- Water quality indices were carried out to evaluate the suitability of surface water to domestic use.
- Surface runoff might significantly impact the water quality.
- High concentration of nitrate in wet season suggests influence of anthropogenic activities on surface water.

GRAPHICAL ABSTRACT

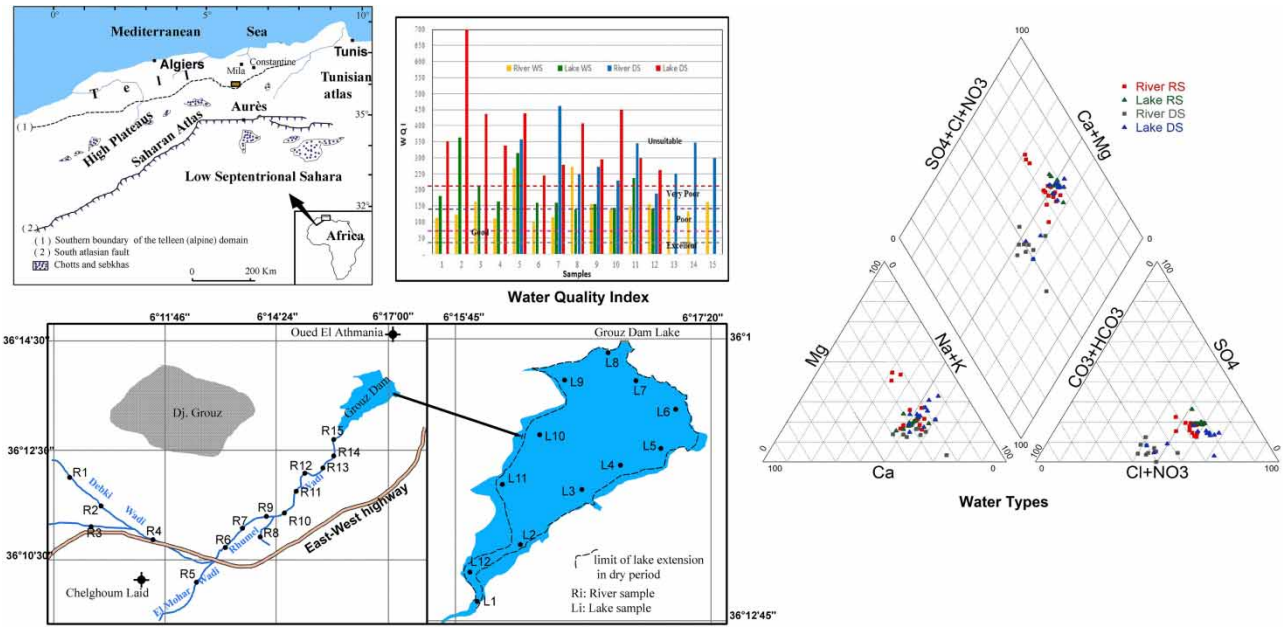

1. INTRODUCTION

If water is an indispensable natural resource essential for all life, development, and security, its availability is increasingly declining due to demand surpassing current supply exacerbated by rapid global population growth, which places additional pressure on this vital resource. Ensuring access to clean water is essential for human communities, significantly contributing to social prosperity and public health (Boretti & Rosa 2019). In this context of increasing demand, maintaining water quality becomes a major concern. Water quality, determined by its composition, is influenced by various natural and anthropogenic factors (Mahaqia *et al.* 2020; Biswas *et al.* 2024; Li *et al.* 2024). Therefore, water chemistry reflects the cumulative effects of these processes, and its composition, in constant flux, reveals the mechanisms that have influenced it (Allia & Lalaoui 2024; Okafor *et al.* 2024). However, its hydrogeochemical evaluation relies largely on comprehensive data relating to water chemistry. Consequently, precise determination of water characteristics is necessary to evaluate potential changes and implement control measures for sustainable use (Qin *et al.* 2019; Liu *et al.* 2020). To manage water resources effectively, it is crucial to understand the hydrogeochemical evolution of water in its natural environment. This knowledge enhances our understanding of hydrochemical systems, aiding in their preservation and protection (Kadam *et al.* 2022; Saha *et al.* 2024).

In Southern Mediterranean countries, such as Algeria, with semi-arid or arid climates, water quality is becoming increasingly critical due to excessive, uncontrolled, and anarchic overexploitation driven by rising demand (Allia *et al.* 2022). An example of this situation is evident in the Upper Kebir Sub-basin in the south Mila district, North East (NE) Algeria. The surface water in this basin is vital for its strategic contribution to the water supply. It serves as a crucial source of potable water for local and regional communities, in addition to supporting the irrigation needs of agriculture across the region. In this area, the Grouz Dam reservoir is a crucial source of water supply for Oued Athmania city and surrounding agglomerations, and it irrigates approximately 5,000 ha of agricultural land (ABH 2014). Nevertheless, these waters are threatened by pollution from urban waste and the use of chemical fertilizers in extensive agriculture. Studies of water quality in the basin reveal high concentrations of ions, primarily due to the geological composition of the watershed, extensive use of fertilizers, and pollution from human activities (Bessaoud *et al.* 2019; Lalaoui *et al.* 2020). In recent decades, climate change has contributed directly or indirectly to the deterioration of water quality in several ways. It has caused high salinization in the water lake of Grouz Dam due to reduced average rainfall and overexploitation. Reduced surface water has led to the concentration of solutes such as chloride and nitrate due to increased evaporation and decreased dilution (El-Hadef El-Okki *et al.* 2015; Allia *et al.* 2018, 2022). Therefore assessments of water resources and sustainability considerations are of vital importance.

The purpose of this study is to characterize surface waters, analyse their spatial–temporal variability, and evaluate their quality for domestic use by analysing physicochemical parameters and using water quality indices such as the water quality index (WQI), pollution index (PI), heavy metal pollution index (HPI), and nitrate pollution index (NPI). Specifically, the objective is to ascertain the hydrochemistry and surface water suitability in the Upper Kebir Sub-basin, identify the controlling processes influencing the region's hydrochemistry, and analyse the spatial–seasonal variability to determine the spatial extent of water quality deterioration in the study area.

2. MATERIALS AND METHODS

2.1. The study area

The Upper Kebir Sub-basin, designated as 10–3 and referred to as the Upper Rhumel Basin, constitutes one of the seven sub-basins within the large Kébir–Rhumel Basin (10) in NE Algeria. Situated in the southern Mila district, it aligns with the upper valley of Rhumel, spanning geographic coordinates along the latitudes 36°08′ –36°15′ N and longitudes 6°10′–6°18′ E (Figure 1), and covers a total surface area of 1,130 km^2. Exhibiting a sub-circular shape, it is enclosed downstream by the eastern end of the mountain Djebel Grouz and is drained by the river of Oued Rhumel. Characterized by a transient West–East flow pattern, it is regulated by the Grouz Dam at Oued Athménia City (Lalaoui *et al.* 2020).

The study area is characterized by a semi-arid continental-type climate with an average annual temperature hovering around 16.43 °C (ranging from −2.1 to 40.2 °C). However, the wet season is from October to May, while the dry season is from June to September. The average annual rainfall is 383.10 mm/a, while the average annual evaporation, runoff, and infiltration are 291.22, 67.28, and 24.60 mm/year, respectively. These values represent approximately 76.01, 17.56, and 6.42% of annual precipitation. The ephemeral rivers crossing the region are Oued Rhumel, Oued El Mohari, and Oued Dekri that flow during the rainy season. The drainage network is quite dense, but the most important watercourse is Oued Rhumel (ABH 2014; Allia & Lalaoui 2024).

This sub-basin is a syncline Mio–Plio–Quaternary plain surrounded by isolated and abrupt reliefs. The geology of the region is marked by the superposition of three litho-stratigraphic units. The basic unit is a Jurassic–Cretaceous neritic carbonate complex, characterized by limestone, dolomitic limestone, and dolomite, with localized occurrences of phosphate deposits. A marly group, dating from the Upper Senonian to the Paleocene age, consisting of marls, overlies this complex as well as marly clays interspersed with evaporated minerals such as gypsum and salts. The uppermost unit consists of heterogeneous detrital Mio–Plio–Quaternary deposits, encompassing red clays transitioning to evaporate. In addition, this unit contains interbedded lacustrine limestone, sandstone, and conglomerate (Villa 1980; Allia *et al.* 2022; Allia & Lalaoui 2024) (Figure 1(c)). The predominant soil type in this area is typically fine alluvial soil, renowned for its high agricultural fertility, particularly suitable for cereals and vegetable cultivation. Nevertheless, the excessive use of chemical fertilizers poses health hazards, leading to reduced crop diversity and nutrient deficiencies resulting from pesticide usage. Hydrogeologically, the study area contains two distinct aquifer systems. One is porous and located within the Mio–Plio–Quaternary formations, while the other is fissured and karstic and found within the Jurassic and Cretaceous carbonate formations (Allia & Lalaoui 2024).

2.2. Sampling analysis of surface water

In order to assess and identify the surface water quality and hydrochemical properties, a detailed field survey was carried out in the study area. Two sampling campaigns were conducted during December–January (rainy or wet season) and August–September (dry season) in the period 2020–2021. A total of 27 sites were sampled (15 sites in the dam lake area and 12 sites along the Oued Rhumel and its main tributary, the Oued Dekri) (Figure 2). It is worth noting that some sites along the Oued Dekri were exclusively sampled during the rainy season due to their dry conditions during the dry season. Standard methods (APHA 2005) were employed during collection and analysis of surface water samples. The water samples were collected in pre-washed 1.5-L polyethylene bottles. For each sampling point, two replicate water samples were collected; one of the bottles was acidified with HNO_3 for cation determinations, while the other was kept unacidified for the anion analyses. These bottles were properly sealed, labelled, and brought to the laboratory for further physicochemical analysis and were stored below 3–5 °C. For all samples, temperature (T°), hydrogen potential (pH), electrical conductivity (EC), and total dissolved solids (TDS) were determined in the field itself with standard field equipment using portable devices (multiparameter SensoDirect 150). The major ions (Ca^{2+}, Mg^{2+}, K^+, CO_3^{2-}, HCO_3^-, SO_4^{2-}, Cl^-, and NO_3^{2-}), total hardness (TH), and total alkalinity (TA) were analysed in the laboratory of Natural Sciences and Materials (LSNM) of Mila University

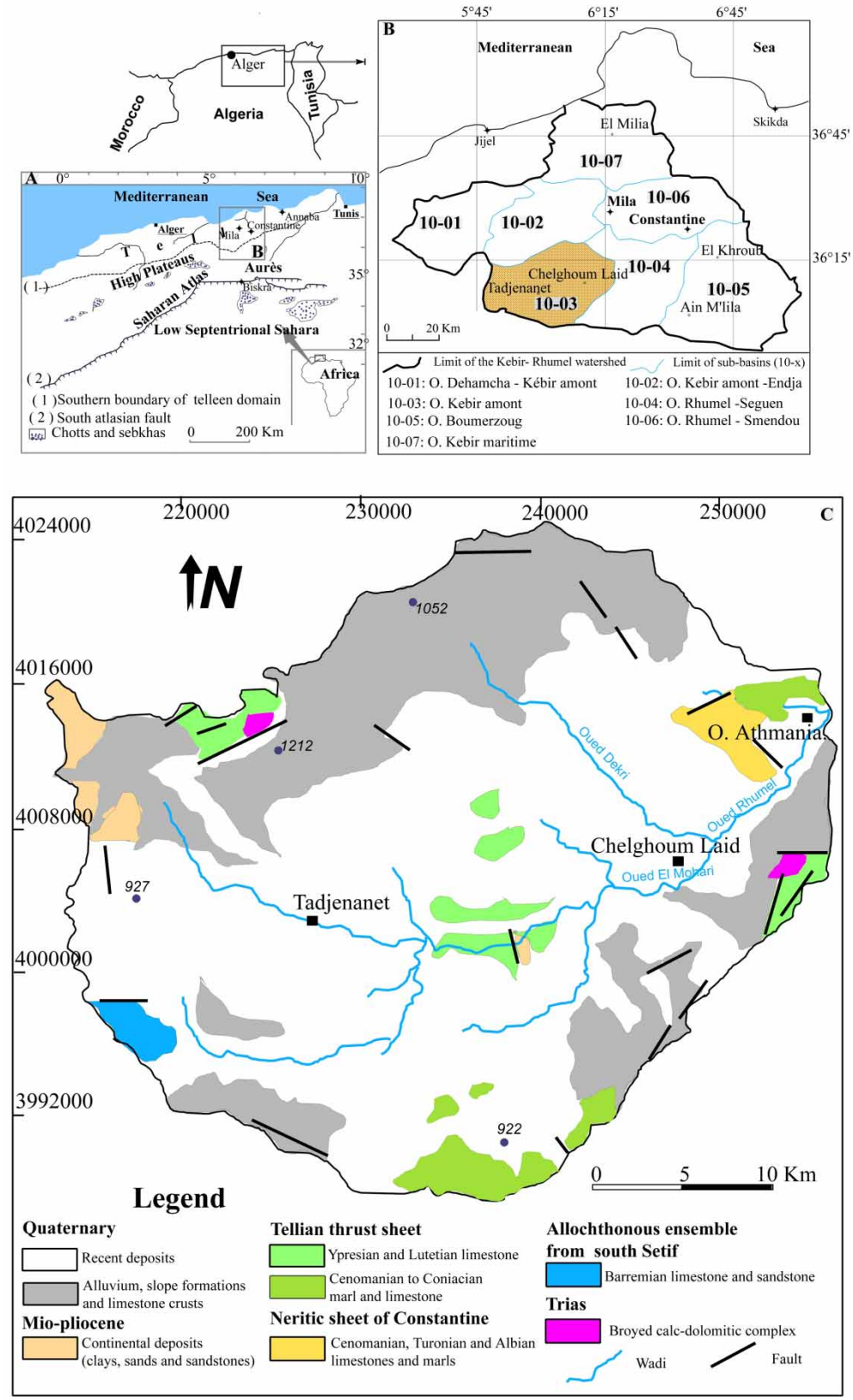

Figure 1 | (a) Major geomorphologic units of North Algeria (Chebbah 2016); (b) Kebir–Rhumel Sub-basins (ABH 2014); (c) Geological map of the study area, redesigned from Setif geological map at 1/200,000 (Villa 1977).

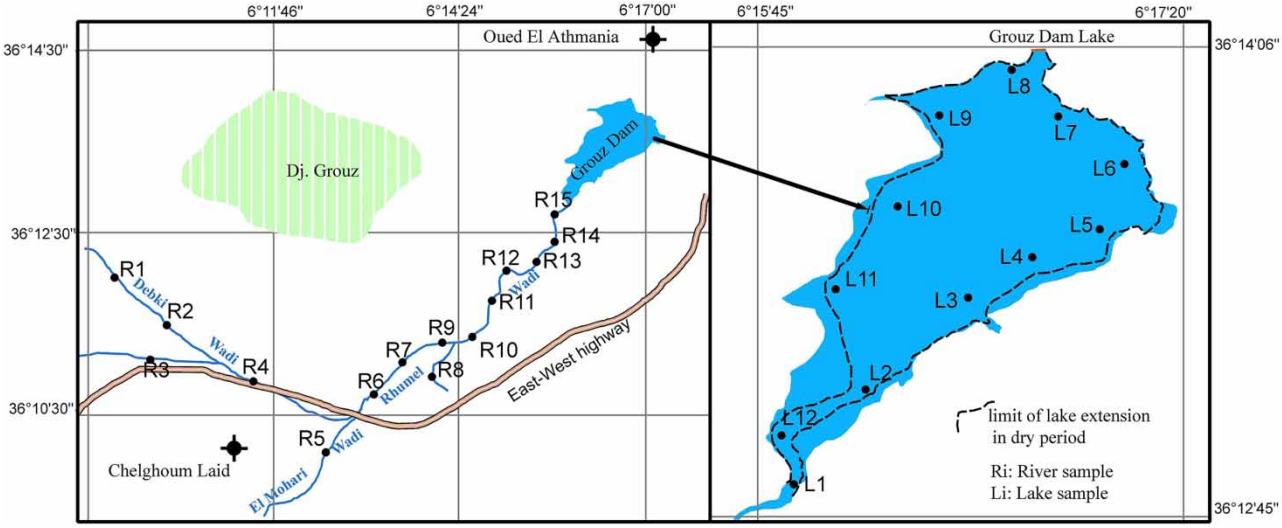

Figure 2 | Map location of samples.

using ion photometers with tablets (Palintest photometer 7,500 and Lovibond photometer MD600). Sodium ion (Na^+) was determined by a flame photometer (Agilent 240/280 Series AA). Sampling point coordinates were recorded using GPS-enabled mobile phone.

2.3. Hydrochemical type and salinization processes of surface waters

2.3.1. Hydrochemical type

Piper diagrams are utilized to graphically represent the chemistry of water samples (Piper 1944). These diagrams facilitate the visualization of the relative concentrations of key ions in the water. They display the percentages of Mg^{2+}, Ca^{2+}, and the combined Na^+ and K^+ cations, along with the percentages of Cl^-, SO_4^{2-}, and the combined HCO_3^- and CO_3^{2-} anions. These six ion groups are plotted on two separate ternary diagrams for cations and anions, which are then integrated into a single rhombus-shaped field for comprehensive analysis. The Piper diagrams were generated using the DIAGRAMME software (Version 6.72).

2.3.2. Salinization processes

Water mineralization is acquired during weathering and water circulation in rocks and soils, where ions are leached and dissolved. Key factors influencing water geochemistry include geological formations, water–rock interactions, ion mobility, and anthropogenic pollution. To determine the origin and processes of natural water mineralization, several ion correlations and ratios including Gibbs' diagrams were used (Chebbah & Allia 2015; Long *et al.* 2018). Gibbs' diagrams help differentiate the effects of weathering, precipitation, and evaporation on natural water composition (Gibbs 1970; Selvakumar *et al.* 2017).

2.4. Quantification of surface water quality

There are several indices for surface water assessment; however, those that were used to assess the surface water acceptance level in the study area were the WQI of Horton (1965), Pollution Index (PI) of Subba Rao (2012), HPI of Mohan *et al.* (1996), and Nitrate Pollution Index (NPI) of Obeidat *et al.* (2012).

WQI was calculated using 22 physicochemical parameters based on the weighted arithmetic indexing method (Galal Uddin *et al.* 2021), using the following equations:

$$\mathrm{WQI} = \sum \mathrm{SI}_i \tag{1}$$

$$\mathrm{SI}_i = W_i \times Q_i \tag{2}$$

$$Q_i = \left(\frac{C_i}{S_i}\right) \times 100 \tag{3}$$

$$\text{and} \quad W_i = \frac{w_i}{\sum w_i} \tag{4}$$

where SI_i is the sub-index of the ith parameter, Q_i is the quality ranting scale, W_i is the relative weight, C_i is the element concentration of the water sample, and S_i is the World Health Organization (WHO) drinking standard.

The summary of the WHO drinking standard, assigned weight (w_i), and relative weight (W_i) are illustrated in Table 1.

PI, like WQI, was calculated using 22 physicochemical parameters based on the weighted arithmetic indexing method by using the following equations:

$$\text{PIS} = \sum_{i=1}^{n} Ow \tag{5}$$

$$\text{Ow} = W_i \times \text{Sc} \tag{6}$$

$$\text{SC} = \frac{C_i}{S_i} \tag{7}$$

where Ow, representing the overall chemical quality of water, is calculated using the W_i parameter and SC the concentration status; and C_i is the concentration of individual chemical variables in each water sample.

Table 1 | The WHO standards for surface water quality parameters and the weight values

Parameters	WHO (2017)	Assigned weight (w_i)	relative weight (W_i)
pH	6.5–8.5	4	0.060606
T (°C)	25	3	0.045455
CE (μs/cm)	1,000	5	0.075758
TDS (mg/L)	500	2	0.030303
TH (mg/L)	200	3	0.045455
TA (mg/L)	200	3	0.045455
Turb (NTU)	5	2	0.030303
Ca (mg/L)	75	3	0.045455
Mg (mg/L)	50	3	0.045455
Na (mg/L)	200	4	0.060606
K (mg/L)	10	3	0.045455
HCO_3 (mg/L)	125	2	0.030303
CO_3 (mg/L)	125	2	0.030303
SO_4 (mg/L)	250 (mg/L)	4	0.060606
Cl (mg/L)	250 (mg/L)	4	0.060606
NO_3 (mg/L)	50	5	0.075758
NH_4 (mg/L)	35	3	0.045455
PO_4 (mg/L)	5	4	0.060606
Fe (mg/L)	0.3	3	0.045455
Al (mg/L)	0.2	2	0.030303
Cu (mg/L)	2	1	0.015152
Mn (mg/L)	0.4	1	0.015152
Total weight		66	1

HPI was calculated using the following equations:

$$\mathrm{HPI} = \frac{\sum W_i * Q_i}{\sum W_i} \tag{8}$$

$$Q_i = \sum \left(\frac{M_i - l_i}{U_i - l_i} \right) \times 100 \tag{9}$$

where Q_i is the sub-index of metal i, W_i is the unit weight of metal i, M_i is the measured concentration of the heavy metal in samples i and l_i, and U_i refers to the lower desirable limit (LDL) and maximum permissible limit (MPL) of ith metal. The sign (–) denotes a numeric difference between the two values regardless of the algebraic sign.

NPI is determined using the following equation:

$$\mathrm{NPI} = \frac{(C_i - \mathrm{HAV})}{\mathrm{HAV}} \tag{10}$$

where C_i represents the measured concentration of nitrate in the sample, while HAV stands for the human acceptable value of nitrate, typically set at 50 mg/L.

3. RESULTS

3.1. Physical–chemical characterization of surface waters

The summary statistical results of the physicochemical parameters and heavy metal contents of the studied waters, during wet and dry seasons, are presented in Table 2.

3.1.1. Temperature (*T*)

Water temperature is a crucial physical parameter for chemical and biochemical reactions, particularly in reservoir water. It affects the hydrogen potential (pH), density, viscosity, gas solubility in water, and the development and growth of living organisms (WHO 2011). An increase in temperature decreases density and viscosity, increases saturated vapour tension at the surface, and reduces gas solubility, promoting self-purification and accelerating sedimentation. Conversely, temperatures below 10 °C slow down chemical reactions in various water treatments (Rodier 2005). Temperatures, measured *in situ* (Table 2), show little variation in surface water temperatures between points during wet and dry periods. The recorded temperatures align with WHO standards (25 °C) during the wet season but exceed them during the dry period in lake waters. These variations correspond to regional climate patterns and daily sampling time lags.

3.1.2. Hydrogen potential

pH is a critical measure as it influences many physicochemical equilibria and interacts with other parameters such as hardness, alkalinity, and temperature (Rodier 2005). It determines the chemical form of elements in water and their transformation from one form to another. Low pH increases the risk of metals being present in a more toxic ionic form, while high pH increases ammonia concentrations. The pH values of natural waters range between 6 and 8.5, decreasing in the presence of organic matter and increasing in the dry season when evaporation is high. Measured pH levels are moderately high and basic, increasing from upstream (river) to downstream (lake) in both seasons. During the dry season, pH levels are higher than during the wet season. Most river water points exceed the desirable pH limit of 8.5 but stay within the MPL of 9.2 recommended by WHO. By contrast, only 50% of lake water samples fall within the desirable limit during the wet period, and 75% exceed the MPL in the dry season, indicating poor water quality, especially in the dry season. The pH increase is due to reduced water quantity from decreased precipitation and increased evaporation, leading to higher ion concentrations and consequently increased salinization of the waters (Amelia 2022).

EC and TDS measure water ability to conduct electricity and its concentration of dissolved substances, respectively. These two closely related parameters indicate water mineralization and pollution levels, which are influenced by multiple factors such as temperature, ion concentration, and the geological formations of watersheds. The analysis of the studied waters reveals that EC and TDS are higher in river water during both seasons, with increased salinity during the dry season due to evaporation. Generally, river waters exhibit higher levels than those of the dam lake, with marked seasonal fluctuations.

Table 2 | Statistics of physicochemical parameters of the surface water samples with WHO (2017) standard values for drinking water quality

	River						Lake							
	Range		MOY		CV%		Range		Mean		CV%		WHO Standards	
	WS	DS	WS	DS	WS	DS	WS	DS	WS	DS	WS	DS	DL	MPL
pH	7.6–9	8.1–9.3	8.1	8.8	5.3	4.9	8–9.0	9–10.7	8.5	10.1	3.7	6.4	6.5–8.5	9.2
T (c°)	13–20	19.5–26.5	14.6	22.7	12.8	9.9	7.5–18	22.8–28.6	12.8	26.2	24.4	8.5	25	25
EC (μs/cm)	865–2,040	2,420–6,750	1,281.9	3,114.0	28.6	42.4	977–1,358	1,943–2,760	1,104.6	2,183	10.6	14.9	900	1,400
TDS (mg/L)	464–1,090	1,300–3,630	682.5	1,663.0	28.8	42.9	522–747	1,010–1,470	593.3	1,146	11.1	14.0	600	900
TH (mg/L)	398–828	400–860	478.1	600.0	21.0	22.1	370–552	320–720	445.8	473.3	11.8	23.9	100	500
TA (mg/L)	252–519	510–840	323.4	714.0	20.7	15.4	238–296	69–800	263.3	273.3	7.2	73.1	200	
Turb (NTU)	1.1–32.3	107–204	12.9	155.5	86.1	44.1	1.7–93.5	101–1,066	43.7	321.6	65.1	86.8	5	10
Ca^{2+} (mg/L)	98–165	80–185	127.9	131.5	17.4	30.6	95–175	44–165	136.6	96.3	16.4	34.0	75	200
Mg^{2+} (mg/L)	42–137	7–70.0	70.5	43.1	42.3	37.9	44–75	46–75	53.8	57.6	14.8	14.8	50	150
Na^{+} (mg/L)	162–272	163.4–296	238.5	222.0	14.8	14.5	242–259	197.2–225	257.7	219.5	1.9	5.1		200
K^{+} (mg/L)	2.9–172.5	56–190	35.4	127.2	132.0	30.1	15–47.5	25–152	20.8	59.1	47.0	84.2	12	
HCO_3^- (mg/L)	196–465	490–808	276.6	665.6	22.4	16.0	188–276	1–42	225.7	296.0	10.1	73.5	125	350
CO_3^{2-} (mg/L)	28–100	20–72	46.8	48.4	35.2	35.2	11–56	0–78	37.7	29.0	36.8	67.9	125	350
SO_4^{2-} (mg/L)	126–284	41.5–160	184.5	77.9	22.4	36.7	190–300	20–180	206.7	107.8	14.6	36.7	200	500
Cl^{-} (mg/L)	360–460	290–525	398.9	394.0	6.9	14.5	400–400	350–400	400.0	389.6	–	5.1	250	600
NO_3^{2-} (mg/L)	13.2–108	0.4–13.6	62.8	2.8	46.1	139.7	52–124	1.2–6.7	76.3	2.4	26.5	61.7	50	
NH_4^{+} (mg/L)	0–0.1	26.2–85.5	0.0	65.1	74.7	30.8	0–0.3	0.5–85.5	0.0	19.2	171.1	175.7	0.1	
PO_4^{3-} (mg/L)	1–27.0	24–39	9.9	29.6	83.6	19.3	3–11.0	1–31.0	5.9	13.0	49.5	102.4	200	
Fe^{2+} (mg/L)	0.1–0.5	0–0.6	0.2	0.3	69.1	60.6	0.1	0.2–1.3	1.0	0.6	251.8	49.8	0.3	
Al (mg/L)	0–0.11	0–0.02	0.024	0.007	122	100	0–0.9	0.1–1.4	0.2	0.5	130.8	93.7	0.2	
Cu (mg/L)	0–0.6	0.1–2.1	0.3	0.9	67.6	69.1	0.1–4.8	0.4–6.4	1.2	2.2	110.6	75.3	2	
Mn (mg/L)	0.002–0.008	0.01–0.36	4.98	33.3	50.7	107	0.0.4–0.02	0.002–0.02	0.007	0.009	74.76	59.87	0.4	

Range: minimum–maximum; MOY, middle of year; CV %, coefficients of variation (%); DL, desirable limits; MPL, maximum permissible limits; EC, TDS, TH, and TA values are at 25 °C.

It should also be noted that the river waters of some tributaries are classified as brackish, and during the dry season, these waters have higher salinity levels, reflecting elevated ion concentrations caused by the dissolution and leaching of watershed terrains.

The TH of water is primarily attributed to its concentration of calcium and magnesium ions. Analysis of the results indicates that TH values are higher during the dry period, with the highest values recorded, particularly, in the river, where 30% of sampled points surpass the MPL set by the WHO. This contrasts with the lake waters, where only 16.67% exceed the limit, particularly at sampling point L1 located at the river mouth, following the reduction in the lake flood zone during the dry season. Conversely, during the wet period, TH values generally remain within the WHO permissible limits.

TA measures the alkalinity of water, which is closely linked to its hardness, and therefore to its corrosive nature and its scale-forming capacity in pipelines. In the waters studied, TA is consistently higher in the river compared to the lake during both seasons. In the river waters, TA increases during the dry season, with very high values recorded. For lake waters, TA only increases at some points. During the dry season, these points effectively become part of the river due to the reduction of the lake's flooded area.

Turbidity measures the cloudiness of water caused by undissolved matter, indicating the quantity of suspended particles. For all analysed samples, turbidity values exceed the MPL recommended by the WHO (10 NTU) during both seasons. The values are higher during the dry period, particularly in the lake at sampling point L2. This point, part of the lake during the wet period, effectively becomes part of the river as the flooded area retreats. Notably, turbidity is consistently higher in the lake than in the river during both seasons.

3.1.3. Main ions in water

3.1.3.1. Calcium. Calcium (Ca^{2+}) is a major component of water hardness, existing mainly as bicarbonates and, to a lesser extent, as sulphates or chlorides. The concentrations of Ca^{2+} are higher during the wet period in the lake waters and during the dry period in the river waters, likely due to the dissolution of gypsum in carbonate formations that form the landforms in the watershed. The average values exceed the WHO desirable limit of 75 mg/L but remain below the MPL of 200 mg/L in both seasons for river and lake waters. The Ca^{2+} levels are generally comparable across the study area, although they are higher in the river waters during the dry season except at some sampling points (R5, R12, R14, and R15). Conversely, Ca^{2+} concentrations decrease in the lake waters during the dry season except at sampling point L12.

3.1.3.2. Magnesium. Magnesium (Mg^{2+}) comes from the dissolution of magnesium-rich and basic rocks, as well as industrial discharges. It is the second contributor to water hardness after calcium. The concentrations of Mg^{2+} in the studied waters are well below the WHO MPL of 150 mg/L, and close to the desirable limit at certain points in both seasons. Maximum concentrations are recorded during the wet period in the river waters, while in the lake, Mg^{2+} concentrations are similar between the two seasons.

3.1.3.3. Sodium. Sodium (Na^{+}), often associated with chlorides and sulphates, comes from the leaching of sodium chloride–rich sedimentary deposits, industrial or domestic wastewater, and fertilized farmland. The concentrations of Na^{+} often exceed the MPL of 200 mg/L, especially during the wet season, except for a few points. Na^{+} contents decrease in the dry season except for one point that records a maximum concentration of 296 mg/L.

3.1.3.4. Potassium. Potassium (K^{+}) concentrations, in the studied samples, exceed the desirable limit of 12 mg/L at most points, especially during the dry season. The points located at the junction of rivers and the lake show high values in the dry season.

3.1.3.5. Bicarbonate. Bicarbonate (HCO_3^-), causing water alkalinity, is unstable in solution and tends to transform into calcium carbonate. HCO_3^- stability is related to water temperature and dissolved carbon dioxide. The concentrations of HCO_3^- in studied waters show values exceeding the WHO MPL of 350 mg/L and are higher during the dry season in the river waters and increase in the lake at certain points connected to the river during the dry season.

3.1.3.6. Carbonate. Like bicarbonate, carbonate (CO_3^{2-}) is an important ion for water alkalinity. CO_3^{2-} levels do not exceed the desirable limit set by the WHO and are well below the MPL of 350 mg/L in all studied waters in both seasons. However, it

should be noted that CO_3^{2-} concentrations fluctuate from one sampling point to another during the dry season. Carbonate variations closely follow those of bicarbonate and alkalinity.

3.1.3.7. Sulphate. Sulphate (SO_4^{2-}) comes from the dissolution of gypsum, anhydrite, and the oxidation of sulphide minerals. Another source can be the infiltration of fertilizers or pesticides. The concentrations of SO_4^{2-} are well below the WHO MPL of 500 mg/L for both waters, with slight variations between the seasons. In the dry season, all points are below the desirable limit of 200 mg/L. In the wet season, values are within the desirable limit except at two points.

3.1.3.8. Chloride. Chloride (Cl^-) mainly comes from the dissolution of saline formations and wastewater contamination, making Cl^- a good tracer of anthropogenic activities. All values exceed the desirable limit of 250 mg/L but remain below the MPL of 600 mg/L, with little variation between the seasons.

3.1.3.9. Nitrate. Nitrate (NO_3^-) in natural waters primarily comes from soil runoff in the watershed due to the natural decomposition of organic nitrogenous matter by microorganisms, converting it to ammonium and then oxidizing to nitrates. The results show a significant decrease in nitrate contents during the dry season compared to the wet season. NO_3^- concentrations are well below the desirable limit (50 mg/L) in the dry season, while about 78% of the samples exceed this limit in the wet season. The high nitrate contents during the wet season are most likely due to wastewater discharge, industrial activity leaks, and agricultural practices resulting from excessive fertilization. The decrease in nitrate levels during the dry season is due to reduced agricultural activity and fertilizer use in the summer.

3.1.3.10. Phosphate. Phosphate (PO_4^{3-}) comes from natural and anthropogenic sources. It is usually responsible for accelerating eutrophication in surface waters and, when exceeding quality standards, indicates faecal contamination leading to microbial proliferation, taste, and colour issues. PO_4^{3-} concentrations are well below the WHO desirable limit of 200 mg/L and higher in river waters than in the lake in both seasons. In river waters, PO_4^{3-} contents increase in the dry season, while in the lake, they decrease to undetectable levels except at certain points connected to the river.

3.1.3.11. Ammonium. Ammonium (NH_4^+) is an indicator of urban pollution and, in surface waters, comes from the excretion of living organisms and the reduction and biodegradation of waste, along with contributions from domestic, agricultural, and industrial sources. NH_4^+ concentrations in the studied waters are below the WHO standard (0.1 mg/L) during the wet season, but significantly exceed this value during the dry season. The lowest NH_4^+ values are recorded during the wet season in both waters and in the lake waters during the dry period. However, the increase in NH_4^+ concentrations at certain points is explained by the lake recession, causing these points to become extensions of the river. They are present in low proportions during the wet season but increase significantly in the dry season, especially in river waters.

The main cations in the river waters are dominated by Na^+ and Ca^{2+} during both seasons, with the following order: $Na^+ > Ca^{2+} > Mg^{2+} > K^+$ during the wet season and $Na^+ > Ca^{2+} > K^+ > Mg^{2+}$ during the dry season. None of the studied samples waters exceeded the MPL recommended by the WHO. The main anions in the river waters are dominated by Cl^- and HCO_3^- during both seasons, with the following order: $Cl^- > HCO_3^- > SO_4^{2-} > NO^{3-} > CO_3^{2-}$ during the wet season and $HCO_3^- > Cl^- > SO_4^{2-} > CO_3^{2-} > NO^{3-}$ during the dry season. Anion concentrations in most samples do not exceed the WHO authorized limits, except for sulphates and nitrates. While the majority of sampled waters do not exceed the WHO permissible reference value for sulphates, the majority of samples exceed the authorized limit of 50 mg/L for nitrates during the wet season. The high nitrate concentrations during the wet season are most likely due to wastewater discharge, industrial activity leaks, and agricultural practices resulting from excessive fertilization. These observations show seasonal and spatial variations of ions in the studied waters, indicating sources of pollution and geochemical processes affecting water quality.

3.1.4. Heavy metals

Heavy metals are present in trace amounts in sediments and naturals waters, and their impact on the environment depends on their concentrations relative to natural levels. These metals come from both natural and anthropogenic sources, including agriculture and urban and industrial discharges, which considerably modify their distribution and often increase their

presence in the environment. In the current study, four elements were analysed [Iron (Fe), Copper (Cu), Manganese (Mn^{2+}), and Aluminium (Al)].

Fe is the fourth most abundant element in the Earth's crust and can enter water from terrain leaching, industrial discharges, and the corrosion of metal pipes. It is essential for various biological processes, including DNA replication, mitochondrial respiration, and oxygen transport, that are crucial for the survival of almost all living organisms. In river waters, Fe levels are below the WHO limit (0.3 mg/L) during the wet season but increase and occasionally surpass the standard in the dry season, particularly at certain points (R5, R7, and R14). In the lake, Fe levels are generally within limits during the wet season except at points L2 and L5, where they rise due to local discharges, and they increase significantly in the dry season.

Cu originates from metal pipe corrosion and industrial, agricultural, and wastewater discharges. Cu levels in lake waters are higher than in the river, increasing during the dry season, with most points exceeding the WHO limit (2 mg/L), notably at L2 with 8.6 mg/L.

Mn exists in multiple oxidation states in water and can cause severe health issues at high levels, such as 'manganism' and reduced IQ in children (Gunnar & Van Dulmen 2007). The Mn levels in both the river and lake waters studied are below the WHO standard (0.4 mg/L) but increase during the dry season.

Al, used in various products and for water treatment (WHO 2017), shows higher concentrations in the lake than in the river waters. Al levels in the river are low during the wet season but rise above the WHO standard (0.2 mg/L) at two points in the dry season. In the lake waters, Al concentrations exceed the standard at two points during the wet season, while during the dry season, they exceed it at most points.

Values in excess of permitted limits for Fe, Cu, and Al are mainly due to industrial discharges and wastewater in the secondary tributaries of the town of Chelghoum Laid, as well as uncontrolled discharges into the waters of the dam lake.

3.2. Surface water types

The graphical representation of major constituents in natural water helps in explaining its hydrochemical characterization, distribution, and evolution. As mentioned previously, Piper diagrams (1944) are utilized to evaluate the variation and the evolution in the hydrochemical facies or types of studied waters. They comprise three components: the lower left ternary plot representing cations (magnesium, sodium plus potassium, and calcium); the lower right ternary plot representing anions (carbonate plus bicarbonate, sulphate, and chloride); and a middle diamond plot, which is a matrix transformation of the two ternary diagrams. The plots display the relative concentrations expressed in milliequivalents of each sample (i.e., the sum of cations = 100 and the sum of anions = 100). The data points in the centre diamond are located by extending the points in the lower triangles to the point of intersection in the centre plot. The ionic concentrations of the sampled surface waters were plotted on the Piper diagram (Figure 3) and revealed that during the wet season, the chemical composition of surface waters predominantly included Na^+–Cl^- type (53.33% of river water, 75% of lake water) indicating the prevalence of alkali metals over alkaline earth metals ($Na^+ + K^+ > Ca^{2+} + Mg^{2+}$) and strong acid anions over weak acid anions ($Cl^- + SO_4^{2-} > HCO_3^- + CO_3^{2-}$). The remaining samples exhibit mixed Ca^{2+}–Mg^{2+}–Cl^- or SO_4^{2+} type (46.67% of river water, 25% of lake water), suggesting a dominance of alkaline earth metals over alkali metals and strong acids over weak acids. However, in the dry season, river waters are classified into Na^+–Cl^- (30%), Ca^{2+}–Mg^{2+}–Cl^- (10%) and Ca^{2+}–Na^-–HCO_3^- (60%) types. Conversely, lake waters exhibit the following types: Na^+–Cl^- (91.66%) and Ca^{2+}–Mg^{2+}–Cl^- or SO_4^{2+} mixed type (8.33%).

3.3. Processes governing surface water chemistry

Water mineralization occurs through weathering and the circulation of water in rocks and soils, where ions are leached and dissolved (Hassen *et al.* 2016). Geological formations, water–rock interactions, ion mobility, and anthropogenic pollution are key factors influencing water geochemistry. Various ion correlations and ratios, such as those depicted in Gibbs' diagrams, are utilized to determine the origin and processes of natural water mineralization (Long *et al.* 2018; Allia & Lalaoui 2024). Gibbs' diagrams help differentiate the effects of weathering, precipitation, and evaporation on natural water composition (Gibbs 1970). The Gibbs' plot (Figure 4) is employed to discern the association of surface water composition with watershed lithology and to represent the source of chemical constituents in surface water. The ratios for cations and anions, such as $Na/(Na^+ Ca)$ and $Cl^-/(Cl + HCO_3)$, plotted against relative values of TDS, reveal precipitation and evaporation dominance processes in most samples from both wet and dry seasons. This behavioural pattern confirms that many surface water samples from agricultural areas exhibit increased salinity due to higher Na and Cl contents relative to the increase in TDS. Additionally, anthropogenic inputs like agricultural fertilizers, mixed canal/river water, and irrigation flows also influence evaporation

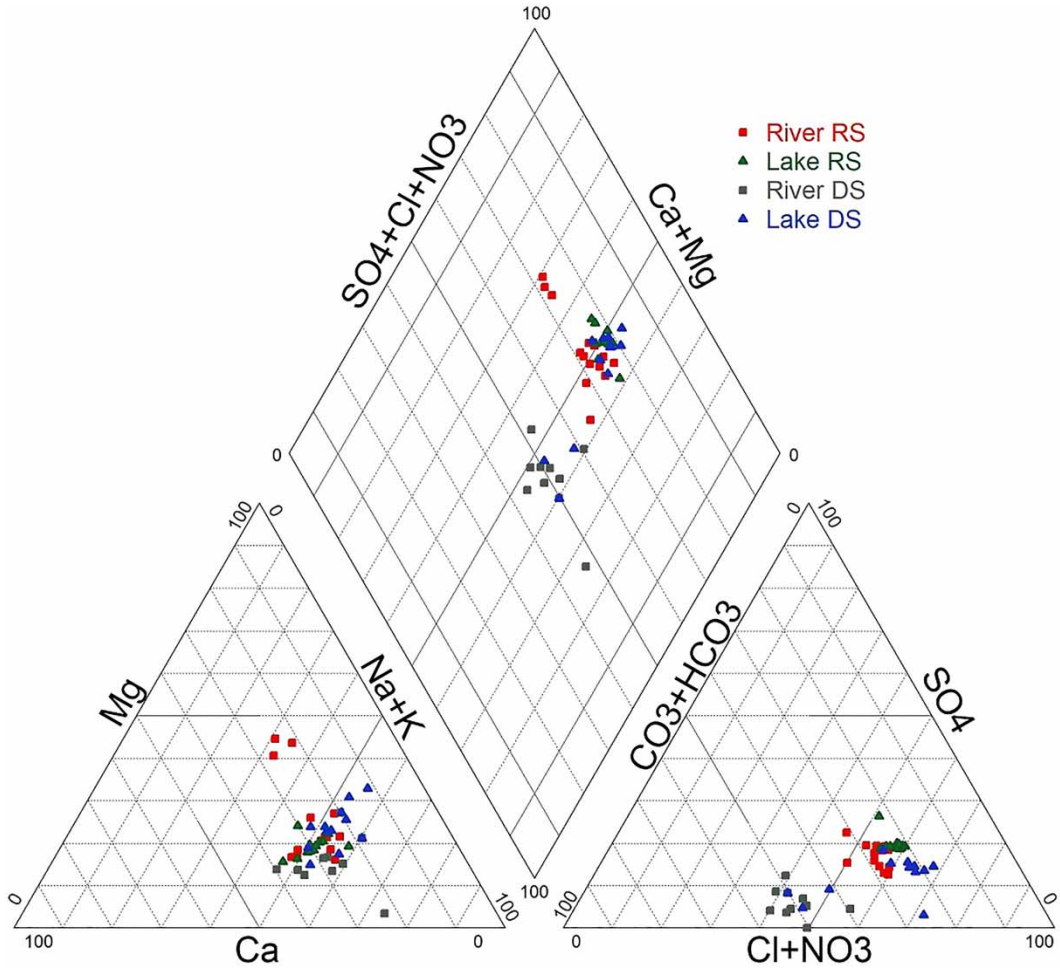

Figure 3 | Piper trilinear diagram of the analysed surface waters; WS, wet season; DS, dry season.

by increasing Na^+ and Cl^-, thereby elevating TDS. This demonstrates that, apart from natural sources, anthropogenic activities play a significant role in determining and dominating changes in the chemical composition of surface water. This, in addition to evaporation and increased aridity in the study area, where, during the year 2021–2022, average precipitation was below the annual average of the last decade, which is 400 mm/year.

3.4. Surface water quality assessment for domestic usage

3.4.1. Water quality index

The water quality in the river and lake varies significantly between the two seasons (Table 3, Figure 5). During the rainy season, only 6.67% of the samples from the river falls into the 'good category' while 80.00% falls into the 'poor category' with 13.33% classified as 'very poor.' Conversely, lake water quality during this season displays 66.67% of samples categorized as 'poor', 16.67% as 'very poor', and 16.67% as 'unsuitable'. However, during the dry season, only 10.00% of the samples from the river are classified as 'poor', while 'very poor' quality dominates at 50.00% followed by 40.00% classified as 'unsuitable'. Similarly, the lake water quality during this period is notably poor, with 41.67% of samples classified as 'very poor' and 58.33% as 'unsuitable'. These results highlight the seasonal fluctuations and the intensification of water quality deterioration during the dry season, emphasizing the need for comprehensive management strategies to preserve these waters. The deterioration of water quality during the dry season is concerning as it may indicate constant sources of pollution and limited dilution capacity. This could affect aquatic biodiversity and human uses of these water resources.

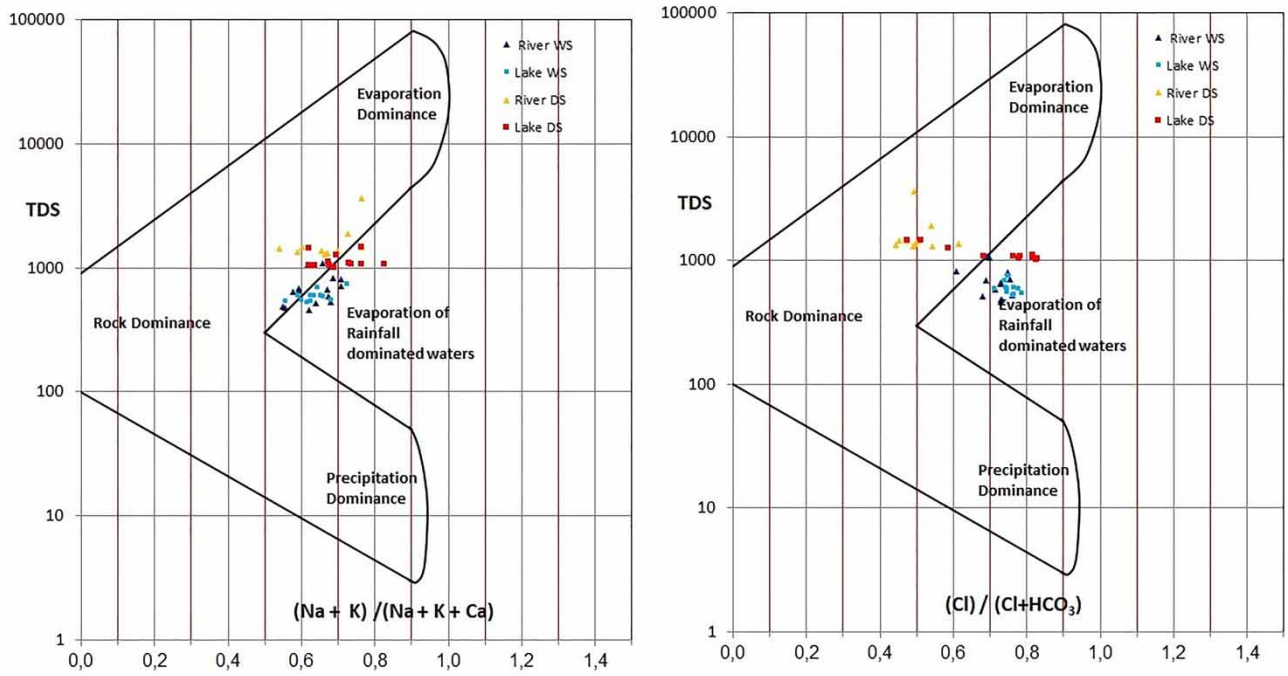

Figure 4 | Gibbs diagrams illustrate the mechanism that controls surface water chemistry; WS, wet season; DS, dry season.

Table 3 | Water quality classifications of waters based on the WQI, PI, NPL, and HPI

			River water		Lake water	
			Number of samples			
Indices	**Water categorization**		**WS**	**DS**	**WS**	**DS**
WQI	<50	Excellent water	–	–	–	–
Horton (1965)	50–100	Good water	1	–	–	–
	100–200	Poor water	12	1	8	–
	200–300	Very poor water	2	5	2	5
	>300	Unsuitable for drinking	–	4	2	7
PI	Less than 1	Insignificant pollution	–	–	–	–
Subba Rao (2012)	From 1 to 1.5	Low pollution	–	–	–	–
	From 1.5 to 2.0	Moderate pollution	1	–	–	–
	From 2 to 2.5	High pollution	–	–	–	–
	Less than 1	Very high pollution	11	10	12	12
NPL	Less than 0	Clean	5	10	–	12
Obeidat *et al.* (2012)	From 0 to 1	Light	8	–	11	–
	From 1 to 2	Moderate	2	–	1	–
	From 2 to 3	Significant	–	–	–	–
	Greater than 3	Very significant	–	–	–	–
HPI	0–25	Excellent	2	1	–	–
Mohan *et al.* (1996)	26–50	Good	9	4	1	2
	51–75	Poor	3	1	7	–
	75–100	Very poor	1	1	2	–
	> 100	Unsuitable	–	3	2	10

3.4.2. Pollution index

The PI serves as a comprehensive metric, assessing the collective impact of various chemical variables on surface water quality. This metric provides a single value that indicates the overall level of natural water pollution (Subba Rao 2012).

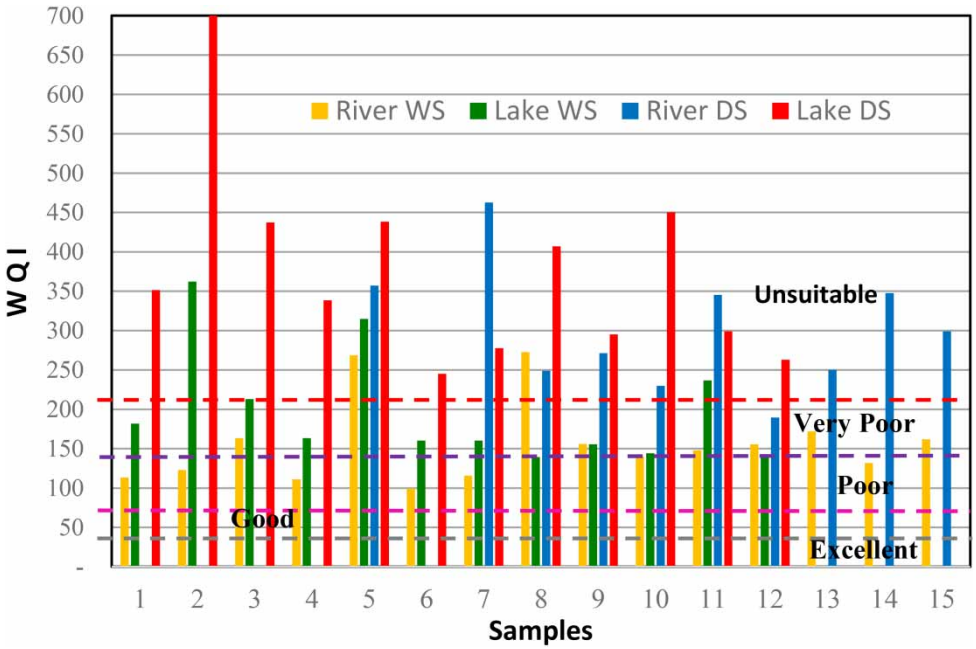

Figure 5 | WQI graphs of studied waters during wet season (WS) and dry season (DS).

The calculated PI values for river waters, as presented in Table 3, range from 1.97 to 4.61 during the wet season, indicating that these waters are moderately to very highly polluted, whereas during the dry season, the PI values range from 2.56 to 5.02, also signifying very high levels of pollution. For lake water, PI values range from 2.67 to 18.57 during the wet season and from 2.89 to 10.33 during the dry season, also indicating very high pollution. PI highlights marked spatial and seasonal variations, indicating significant pollution levels in the waters analysed, particularly the lake waters. It reveals a critical pollution level during the dry season. Seasonal variations in pollution could be attributed to runoff and increased human activity, such as urban discharges and agricultural practices involving excessive fertilizer use, as well as geological attributes during the wet season. The persistence of high pollution levels in lakes is likely due to their stagnant nature, leading to the accumulation of pollutants from reduced water input and increased evaporation during the dry season.

3.4.3. Heavy metals pollution index

The HPI was computed using Equations (8) and (9) for four heavy metals. The results reveal that the HPI of the river water ranges from 21.38 to 81.46 (mean: 41.99) during the wet season and from 16.08 to 219.58 with an average of 79.95 during the dry season. For lake water, the HPI ranges from 40.42 to 1827.46 with an average of 226.99 during the wet season, and during the dry season, the HPI ranges from 37.88 to 677.67 with a mean of 262.71. Surface water samples were classified into five classes based on the HPI values: excellent (0–25), good (26–50), poor (51–75), very poor (75–100), and unsuitable (>100) (Basahi *et al.* 2018). During the wet season, rivers generally have low HPI, indicating good water quality (average: 41.99). During the dry season, while the average remains lower than that of the lake water, some rivers (like R7) show high pollution spikes (max HPI = 219.58). During the wet season, the lake exhibits a wide variation in water quality with HPIs reaching very high levels (max HPI = 1,827.46 for L5) indicating severe pollution problems. During the dry season, lakes continue to show high pollution levels (main: 262.71), although slightly lower than during the wet season. Generally, rivers exhibit better water quality compared to lakes with lower HPI values. The dry season increases pollution in some rivers but not as dramatically as in lakes. Lake water samples in this study also revealed much higher pollution levels, especially during the wet season with extreme variations. The dry season reduces pollution in some points, but the water quality remains concerning.

3.4.4. Nitrate pollution index

NPI is a very important indicator for determining water pollution with nitrates in the polluted water resulting from human activities. It provides an indication of the level of nitrate pollution based on the nitrate concentration in surface water compared with a health recommended value (Obeidat *et al.* 2012). The results reveal that the HPI of the river water ranges from −0.736 to 1.16 during the wet season and from −0.992 to −0.727 during the dry season. For the lake water, the HPI ranges from 0.04 to 1.48 in the wet season, and during the dry season, the HPI ranges from −0.976 to −0.867.

The spatio-seasonal disparity observed in Na^+ levels may be due to increased runoff and human activities during the wet season, leading to elevated nitrate concentrations. Conversely, the decrease noted during the dry period could be attributed to the reduction in runoff and agricultural activities during this season.

4. CONCLUSIONS

The analyses of physicochemical parameters and heavy metal contents in the waters studied revealed significant impacts on water quality due to both natural processes and anthropogenic activities, exacerbated by climatic conditions. The assessment highlights substantial seasonal fluctuations in water quality, with a marked deterioration during the dry season. Rivers exhibit better overall water quality compared to lakes, which show extreme pollution levels, especially for chloride, sodium, nitrate, and heavy metals, during the wet season. The persistent pollution and reduced dilution capacity during the dry season harm aquatic life and human water consumption.

The results underscore the urgent need for comprehensive water quality monitoring and vigorous pollution control measures. Essential actions include implementing innovative water management strategies, advanced monitoring systems, sustainable agricultural practices, and improved wastewater treatment. Community engagement and awareness programs are also crucial. Prioritizing these initiatives will protect aquatic ecosystems, ensure clean water availability for future generations, and promote community health and wellbeing. Sustainable water resource management is a collective responsibility vital for environmental equilibrium and a resilient future.

AUTHOR CONTRIBUTIONS

Collective work.

DATA AVAILABILITY STATEMENT

All relevant data are included in the paper or its Supplementary Information.

CONFLICT OF INTEREST

The authors declare there is no conflict.

REFERENCES

ABH – Hydrographic Basins Agency. 2014 *Le Bassin du Khébir Rhumel*. Cahiers de l'agence (The Kebir-Rhumel basin, Agency Notebooks), N° 8, Alger, Algeria.

Allia, Z. & Lalaoui, M. 2024 Formation mechanism of hydrochemical and quality evaluation of shallow groundwater in the upper Kebir sub-basin, Northeast Algeria. *J. Groundw. Sci. Eng.* **12** (1), 78–91. http://gwse.iheg.org.cn/en/article/doi/10.26599/JGSE.2024.9280007.

Allia, Z., Chebbah, M. & Ouamane, A. 2018 Analyse et évaluation de la qualité des eaux du système aquifère mio-pliocène dans le Zab Chergui, Bas Sahara Septentrional (Analysis and assessment of water quality of the mio-pliocene aquifer system in the Zab Chergui, Lower septentrional Sahara). *Courrier du Savoir, Univ Biskra, Algérie* **26**, 235–244. Available from: https://revues.univ-biskra.dz/index.php/cds/article/view/3938.

Allia, Z., Lalaoui, M. & Chebbah, M. 2022 Hydrochemical assessment for the suitability of drinking and irrigation use of surface water in Grouz Dam Basin, Northeast Algeria. Sustain. *Water Resour. Manag.* **8** (88), 3–16. https://doi.org/10.1007/s40899-022-00663-8.

Amelia, J. 2022 Effects of climate change on oceans. *J. Climatol. Weath Forecast.* **10** (11), 001–003. doi:10.35248/2332-2594.22.10(11).341.

APHA 2005 *Standard Methods for Examination of Water and Wastewater*, 21st edn. American Public Health Association, Washington, DC.

Basahi, J. M., Milad, H. Z. & Rajmohan, M. N. 2018 Effect of flash flood on trace metal pollution in the groundwater – Wadi Baysh Basin, western Saudi Arabia. *J. Afr. Earth Sci.* **147**, 338–351. https://doi.org/10.1016/j.jafrearsci.2018.06.032.

Bessaoud, O., Pellissier, J. P., Rolland, J. P. & Khechimi, W. 2019 *Rapport de Synthèse sur L'agriculture en Algérie (Synthesis Report on Agriculture in Algeria)*. CIHEAM-IAMM, Montpellier, France.

Biswas, A., Debnath, P., Roy, S., Bhattacharyya, S., Mitra, S. & Chaudhuri, P. 2024 Spatio-temporal variation in water quality due to the anthropogenic impact in Rudrasagar Lake, a Ramsar site in India. *Environ. Monit. Assess.* **196**, 598. https://doi.org/10.1007/s10661-024-12736-6.

Boretti, A. & Rosa, L. 2019 Reassessing the projections of the world water development report. *npj Clean Water* **2** (15), 1–6. https://doi.org/10.1038/s41545-019-0039-9.

Chebbah, M. 2016 A Miocene-restricted platform of the Zibane zone (Saharan Atlas, Algeria), depositional sequences and paleogeographic reconstruction. *Arab. J. Geosci.* **9**, 151. https://doi.org/10.1007/s12517-015-2132-9.

Chebbah, M. & Allia, Z. 2015 Geochemistry and hydrogeochemical process of groundwater in the Souf valley of Low Septentrional Sahara. Algeria. *Afr. J. Environ. Sci. Technol.* **9** (3), 261–273. https://doi.org/10.5897/16-0231-9.

El-Hadef El-Okki, M., Sahli, L., Bentellis, A., Azzoug, R., Laing, G. D. & Rached, O. 2015 Assessment of metal contamination in soil banks of the Rhumel Wadi (Northeast Algeria). *Toxicol. Environ. Chem.* **98** (1), 53–63. https://doi.org/10.1080/02772248.2015.1101115.

Galal Uddin, M., Nash, S. & Olbert, I. A. 2021 A review of water quality index models and their use for assessing surface water quality. *Ecol. Indic.* **122** (107218), 1–21. https://doi.org/10.1016/j.ecolind.2020.107218.

Gibbs, R. J. 1970 Mechanisms controlling world water chemistry. *Science* **170**, 1088–1090.

Gunnar, M. R. & Van Dulmen, M. H. M. 2007 Behavior problems in postinstitutionalized internationally adopted children. *Dev. Psychopathol.* **19** (1), 129–148. https://doi.org/10.1017/S0954579407070071.

Hassen, I., Hamzaoui-Azaza, F. & Bouhlila, R. 2016 Application of multivariate statistical analysis and hydrochemical and isotopic investigations for evaluation of groundwater quality and its suitability for drinking and agriculture purposes: Case of Oum Ali-Thelepte aquifer, central Tunisia. *Environ. Monit. Assess.* **188** (135), 1–20. https://doi.org/10.1007/s10661-016-5124-7.

Horton, R. K. 1965 An index number system for rating water quality. *J. Water Pollut. Control Fed.* **37** (3), 300–306. Available from: http://www.jstor.org/stable/1730827.

Kadam, A., Wagh, V., Jacobs, J., Patil, S., Pawar, N., Umrikar, B., Sankhua, R. & Suyash Kumar, S. 2022 Integrated approach for the evaluation of groundwater quality through hydro geochemistry and human health risk from Shivganga river basin, Pune, Maharashtra, India. *Environ. Sci. Pollut. Res.* **29**, 4311–4333. https://doi.org/10.1007/s11356-021-15554-2.

Lalaoui, M., Allia, Z. & Chebbah, M. 2020 Hydrochemical processes and suitability assessment of surface water in the Grouz Dam Basin, Northeast Algeria. *J. Fundam. Appl. Sci.* **12** (3), 1452–1474. https://doi.org/10.4314/jfas.v12i3.29.

Li, Z., Li, J., Huang, J. & Li, Y. 2024 Nitrate contamination in groundwater and its health risk assessment: A case study of Quanzhou, a typical coastal city in Southeast China. *Environ. Earth Sci.* **83**, 331. https://doi.org/10.1007/s12665-024-11608-z.

Liu, J., Zhao, D., Mao, G., Cui, W., Chen, H. & Yang, H. 2020 Environmental sustainability of water footprint in Mainland China. *Geogr. Sustain.* **1** (1), 8–17. https://doi.org/10.1016/j.geosus.2020.02.002.

Long, D. T., Pearson, A. L., Voice, T. C., Polanco-Rodriguez, A. G., Sanchez-Rodriguez, C., Xagoraraki, I., Concha-Valdez, F., Puc-Franco, M., Lopec-Cetz, R. & Rzotkiewicz, A. 2018 Influence of rainy season and land use on drinking water quality in a karst landscape, State of Yucatan, Mexico. *Appl. Geochem.* **98**, 265–277. doi:10.1016/j.apgeochem.2018.09.020.

Mahaqia, A., Moheghyb, M. A., Moheghic, M. M., Mehiqid, M. & Zandvakili, Z. 2020 Environmental hydrogeochemistry characteristics, controlling factors and groundwater quality assessment in W Afghanistan. *Water Resour.* **47** (2), 325–335. https://doi.org/10.1134/S0097807820020104.

Mohan, S. V., Nithila, P. & Reddy, S. J. 1996 Estimation of heavy metal in drinking water and development of heavy metal pollution index. *J. Environ. Sci. Health, A* **31**, 283–289. https://doi.org/10.1080/10934529609376357.

Obeidat, M. M., Awawdeh, M., Al-Rub, F. A., Al-Ajlouni, A., 2012 An innovative nitrate pollution index and multivariate statistical investigations of groundwater chemical quality of Umm Rijam Aquifer (B4), North Yarmouk River Basin, Jordan. In: *Water Quality Monitoring and Assessment* (Voudouris, K. & Voutsa, D., eds). IntechOpen, pp. 169–188.

Okafor, C. O., Ude, U. I., Okoh, E. F. N. & Eromonsele, B. O., 2024 Safe drinking water: The need and challenges in developing countries. In: *Water Quality – New Perspectives* (Dincer, S., ed.). IntechOpen. doi:10.5772/intechopen.108497.

Piper, A. M. 1944 Graphic procedure in the geochemical interpretation of water analyses. *Trans. Am. Geophys. Union.* **25** (6), 914–923. https://agupubs.onlinelibrary.wiley.com/doi/10.1029/TR025i006p00914.

Qin, C., Zhu, K., Chiariello, N. R., Field, C. B. & Peay, K. G. 2019 Fire history and plant community composition outweigh decadal multi-factor global change as drivers of microbial composition in an annual grassland. *J. Ecol.* **108** (2), 1–15. https://doi.org/10.1111/1365-2745.13284.

Rodier, J. 2005 L'analyse de l'eau, eaux naturelles, eaux résiduaires, eau de mer, chimie, physico-chimie, microbiologie, biologie, interprétation des résultats (Water Analysis, Natural Water, Wastewater, Seawater, Chemistry, Physico-Chemistry, Microbiology, Biology, Interpretation of Results). Dunod (Ed.), Paris, France.

Saha, A., Pal, S. C., Resa Md, A., Islam, T., Islam, A., Alam, A. & Islam, K. 2024 Hydro-chemical based assessment of groundwater vulnerability in the Holocene multi-aquifers of Ganges delta. *Sci. Rep.* **14**, 1265. https://doi.org/10.1038/s41598-024-51917-8.

Selvakumar, S., Chandrasekar, N. & Kumar, G. 2017 Hydrogeochemical characteristics and groundwater contamination in the rapid urban development areas of Coimbatore. India. *Water Resour. Ind.* **17** (2), 26–33. https://doi.org/10.1016/j.wri.2017.02.002.

Subba Rao, N. 2012 PIG: A numerical index for dissemination of groundwater contamination zones. *Hydrol. Processes.* **26**, 3344–3350. https://doi.org/10.1002/hyp.8456.

Villa, J. M. 1977 *Carte Géologique de Sétif au 1/200 000 (Geological map of Sétif at 1/200 000)*. SONATRACH Publication, Algérie.

Villa, J. M. 1980 *La Chaîne Alpine D'Algérie Orientale et des Confins Algéro-Tunisiens (Alpine Chain of Eastern Algeria and the Algerian-Tunisian Border). Thèse Docteur ès Sciences*, Paris VI, France.

WHO 2011 *World Health Organization Guidelines for Drinking Water Quality*, 4th edn. Incorporating the First and Second Addendum, Vol. 1. Recommendation, World Health Organization, Geneva.

WHO 2017 *World Health Organization Guidelines for Drinking-Water Quality*, 4th edn. Incorporating the First Addendum. World Health Organization, Geneva.

First received 15 June 2024; accepted in revised form 29 July 2024. Available online 6 August 2024